Strain-Induced Martensitic Transformation in Fatigued Cast Co-Cr-Mo Alloy Used for Surgical Implants

L. Z. Zhuang and E. W. Langer, Technical University of Denmark, Department of Metallurgy, DK-2800 Lyngby, Denmark

Introduction

In certain austenitic steels, the drastic influence of martensitic transformation on their mechanical properties is well established. The structural and kinetic features of martensitic transformation have been of great interest in relation to the strengthening behaviour of alloys. Therefore, many studies have been carried out on this aspect of phase transformation in various metals and steels (1-20). Most of the current investigations have drawn the attention to the fcc to hcp martensitic transformation because it is associated with a rather simple transformation mode as compared with those for fcc to bcc transformations and other more complex transformations. Numerous approaches have been used to establish mechanisms of the fcc to hcp martensitic transformation, especially concerning nucleation mechanisms of martensite or the formation of martensite's embryos (1-5, 21-27).

As for fcc to hcp martensitic transformations, the nucleation of hcp platelets has been suggested to occur due to overlapping of stacking faults, such nucleation is accelerated by the low stacking fault energy (6-8). Therefore, it has been pointed out that stacking faults in an fcc austenite play an important role in this phase transformation. However, the relationship between stacking faults and the formation mechanism of hcp phase is still unclear. The following two overlapping processes of stacking faults are expected to occur: a) regular, and b) irregular overlapping of stacking faults. Most of the present models support that the fcc to hcp transformation occurs through regular overlapping process of stacking faults (the former category), i.e. the stacking faults are formed on every other close packed plane (4, 5, 23).

Martensitic transformation in the fcc austenitic alloys can be affected by the application of stress, plastic strain and deformation (5-8, 12, 14, 28-34). It is reported that the strain-induced martensitic transformation is identical with the thermally induced martensitic transformation, including the transformation temperature, the morphology (appearance of the interphase boundaries) as well as the volume fraction of transformed martensite.

Although the spontaneous fcc to hcp transformation in Co-Cr-Mo surgical implant alloy introduced by various heat treatment schemes has been studied by many authors (16-20), no publications seem to have dealt with the strain-induced fcc to hcp phase transformation in this alloy system. Moreover, it has been shown that Co-Cr-Mo alloy has a rather low value of the intrinsic stacking fault energy which facilitates the formation of high density of stacking faults and promotes strain-induced martensitic transformation. It also has been shown that in Co-base alloys, the intrinsic stacking fault energy was strongly dependent upon composition (35), as in some other alloy systems (36).

The purpose of this paper is to give a fuller account of the experimental results in the cast Co-Cr-Mo alloy and to discuss the influence of the stacking fault energy on the strain-induced fcc to hcp martensitic transformation by means of alloying the base alloy with nickel addition at various levels. The influence of the phase transformation on the fatigue behaviour, especially the fatigue fracture feature, of the cast Co-Cr-Mo alloy is also discussed.

Materials and Experimental Procedure

Cast Co-Cr-Mo alloy, commercially known as Vitallium or H.S.21 and its modified versions by alloy additions with nickel and some trace elements, Al, Ti, and B, are studied. Alloys are prepared by vacuum induction melting and cast in sand molds with air cooling. The chemical compositions of the alloys are shown in Table 1. Specimens are mechanically tested and structurally examined in the as-cast condition. Individual specimens with dimension of 85x20x30 mm are cast and used for mechanical testing. The as-cast Co-Cr-Mo alloys exhibit a typical microstructure, namely a cored cobalt-rich fcc matrix with interdendritic precipitates and grain boundary precipitates, a coarse dendritic structure with a grain size of about 400 μm is obtained (37).

Table 1. Composition of as-cast alloys used in the present study

Alloy No.	Chemical composition (wt.%)										
	Cr	Mo	Ni	C	Fe	Si	Mn	Co	Ti	Al	B
1	29.07	6.69	-	0.16	0.08	0.05	0.10	bal.	-	-	-
2	27.59	6.49	4.28	0.15	0.08	0.06	0.09	bal.	-	-	-
3	26.24	6.13	9.03	0.15	0.08	0.05	0.09	bal.	-	-	-
4	28.84	6.35	-	0.16	0.06	0.08	0.10	bal.	0.12	0.11	0.01
5	27.40	6.23	4.50	0.16	0.06	0.08	0.10	bal.	0.11	0.11	0.01
6	25.71	5.98	9.48	0.15	0.05	0.07	0.09	bal.	0.11	0.11	0.01

Fatigue testing is conducted using an Instron testing machine (Model-1342) at room temperature, 10 Hz and load ratio R = 0.1 with a stress intensity factor range, ΔK, between about 20 and 50 MPa$\sqrt{m}$. Constant-load-amplitude fatigue crack growth rates (38) are determined using standard three-point bend specimens (39) with S = 64 mm, W = 16 mm, B = 8 mm and a total specimen length L = 80 mm, machined from the original castings.

After fatigue testing, the specimens are sectioned beneath the fracture surface for transmission electron microscopy studies. Transmission electron microscopy is performed using disc-shaped specimens of 3 mm in diameter. They are finally thinned by jet polishing in an electrolyte of 10 pct perchloric acid + 20 pct ethanol + 70 pct butanol by volume, at temperatures between -20°C and -30°C throughout thinning and at a potential of 30V. The specimens are examined in Philips EM301 transmission electron microscope operating at 100KV.

Results and Discussion

By TEM examinations and selected-area electron diffraction analysis, it is revealed that the localized fcc to hcp transformed martensites in the thin layers close to the fracture surface of fatigued specimens can be observed only in the materials of Alloy No.1 and No.4 as listed in Table 1, corresponding to the base alloy and the modified alloy with no nickel addition. This could be interpreted in terms of the effects of stacking fault energy (chemical composition) on the fcc to hcp martensitic transformation.

Plate-like structure of cyclic strain-induced martensite in Fig.1 shows a typical example of ε-phase plates. The classical orientation relationship between austenite matrix and hcp martensite, i.e. $(111)_{fcc} \| (0001)_{hcp}$ and $\langle 1\bar{1}0\rangle_{fcc} \| \langle 11\bar{2}0\rangle_{hcp}$, is indicated by the corresponding selected-area electron diffraction pattern which is included in Fig. 1. The presence of streaks in the SADP lying in direction in the basal plane of the ε-crystal structure results from the small dimension of the parallel thin ε-phase lamellae on the basal plane $(0001)_{hcp}$.

Fig. 2 shows a TEM micrograph of the base alloy taken by the incident beam direction along $[0001]_{hcp}$. It is seen that the fcc to hcp martensitic transformation occurs only on one of the $(111)_{fcc}$ planes. This is rather different from the microstructure observed in thermally induced fcc to hcp martensitic

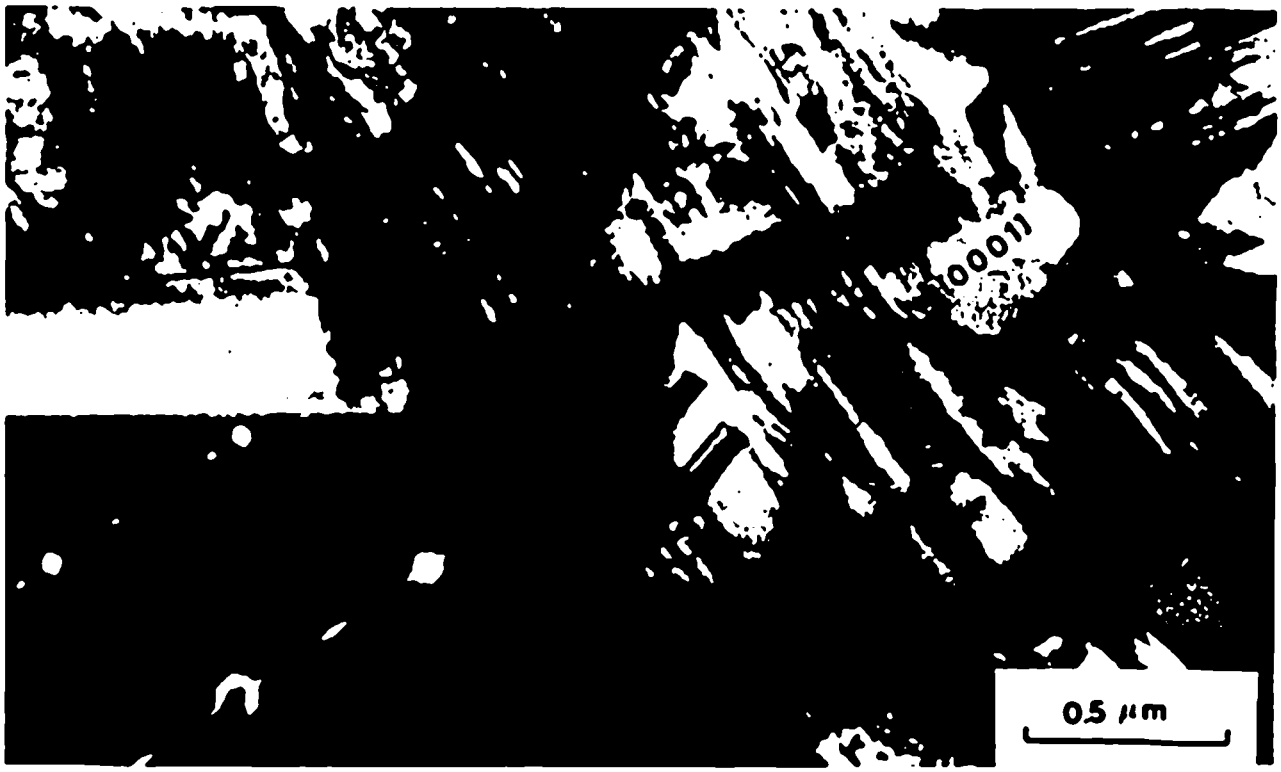

Fig. 1 TEM micrograph of the base alloy after fatigue testing showing the strain-induced ε-phase plates. Beam direction along $[2\bar{1}\bar{1}0]_{hcp} \parallel [110]_{fcc}$.

Fig. 2 Bright field TEM micrograph of the base alloy after fatigue testing showing that the strain-induced martensitic transformation takes place only on one A of the $\{111\}_{fcc}$ planes. Beam direction along $[0001]_{hcp}$.

Fig. 3 Bright field TEM micrograph of the base alloy after fatigue testing showing the strain-induced ε-crystal nucleated at a stacking fault intersection node and with plate structure along two directions. Beam direction along $[10\bar{1}1]_{hcp}$.

transformation. If Shockley partial dislocations form and extend on every other layer in austenite, the stacking faults would pile up to form hcp ε-phase. It is possible in the thermally induced transformation of fcc to hcp that the cooperative movements of all types of partial dislocations with different Burgers vectors of type $1/6\langle 11\bar{2}\rangle$ on the $(111)_{fcc}$ could be carried into execution. When the ε-phase is strain-induced, dislocation motion is governed by the critical resolved shear stress as determined by geometrical considerations including the applied stress axis. Therefore, it seems very likely that only a single type of partial dislocation is active in a given slip system, resulting in the phase transformation taking place only on the plane where the critical resolved shear stress condition is met.

The fcc to hcp transformation is favoured to develop at stacking fault intersection sites where a higher local strain could be provided. In this case, it is possible for the transformation to occur on more than one $(111)_{fcc}$ planes. Martensitic transformation nucleated by stacking fault intersections in the base alloy is shown in Fig. 3 to 5. Fig. 3 shows a transformed region with plate-like structure along two directions taken by the incident beam direction along $[10\bar{1}1]_{hcp}$. Plate-like structure in direction A in Fig. 4, is a fully transformed plate, while in direction B only partly developed. It is noted that the microstructure of ε-crystals at the intersection sites shows a rather highly distorted appearance of the interphase boundaries related to a large accommodation strain at the intersection nodes. A dark field image of hcp reflection with $\vec{g} = [10\bar{1}0]$ is shown in Fig. 5. It is seen in this micrograph that a narrow branch structure (marked M) is also already transformed to thin ε-phase crystals.

Fig. 4 Bright field TEM micrograph of the base alloy after fatigue testing showing a fully transformed ε-phase plate in direction A and a partly developed plate in direction B which is nucleated on the large plate. Beam direction along $[\bar{1}2\bar{1}3]_{hcp}$.

Fig. 5 Dark field TEM image of an hcp reflection with $\vec{g}=[10\bar{1}0]$ showing the strain-induced martensite plates and a thin ε-crystal in the base alloy after fatigue testing. Beam direction along $[\bar{1}2\bar{1}3]_{hcp} \| [10\bar{3}]_{fcc}$.

Fig. 6 Bright field TEM micrograph of the modified alloy with no Ni after fatigue testing showing similar morphology of the strain-induced ε-phase as shown in the base alloy. Beam direction along $[0001]_{hcp}$.

Fig. 7 Bright field TEM micrograph of the modified alloy with no Ni after fatigue testing showing the strain-induced ε-plate structure and overlapping stacking faults. Beam direction along $[\bar{2}110]_{hcp}$.

The fcc to hcp martensitic transformation is also observed in the modified alloy with no nickel addition (Alloy No.4). TEM micrographs of fcc + hcp mixed structure in this alloy are shown in Fig.6 and Fig.7. In Fig.6, a microstructure with parallel ε-plates surrounded by the fcc matrix with high density of stacking faults is seen. Plate-like structure, running from the lower right to the upper left side in Fig. 7, are the thin ε-phase plates. The band-structure in the lower left region is identified as overlapping stacking faults.

Observations of microstructures of the modified alloys with nickel additions (Alloy No.2, 3, 5, and 6) by transmission electron microscopy reveal that there are no cyclic strain-induced fcc to hcp martensitic transformation taking place in the fatigue tested specimens. In all cases, only a high density of stacking faults and the intersections of stacking faults can be observed. The structure of overlapping stacking faults, which can be considered as to be precursors to hcp formation, is seldom seen in these alloys. A TEM micrograph of the alloy 5 with 4.5%wt nickel addition after fatigue tested is shown in Fig. 8, in which a typical stacking fault intersection structure as frequently observed in the cast Co-Cr-Mo alloy is illustrated. Similar microstructures are observed in other alloys with nickel additions up to about 10%wt.

It is well known that regions of hcp martensite can be formed by intrinsic faulting on every alternate {111} plane in the fcc lattice, as suggested by most of the models. Therefore, the fcc and hcp structures are interrelated, each being obtained by an appropriate stacking sequence of close packed planes of atoms, and the fcc/hcp boundaries are generally planar with matching close packed planes at the long straight interfaces and are coherent in nature. The

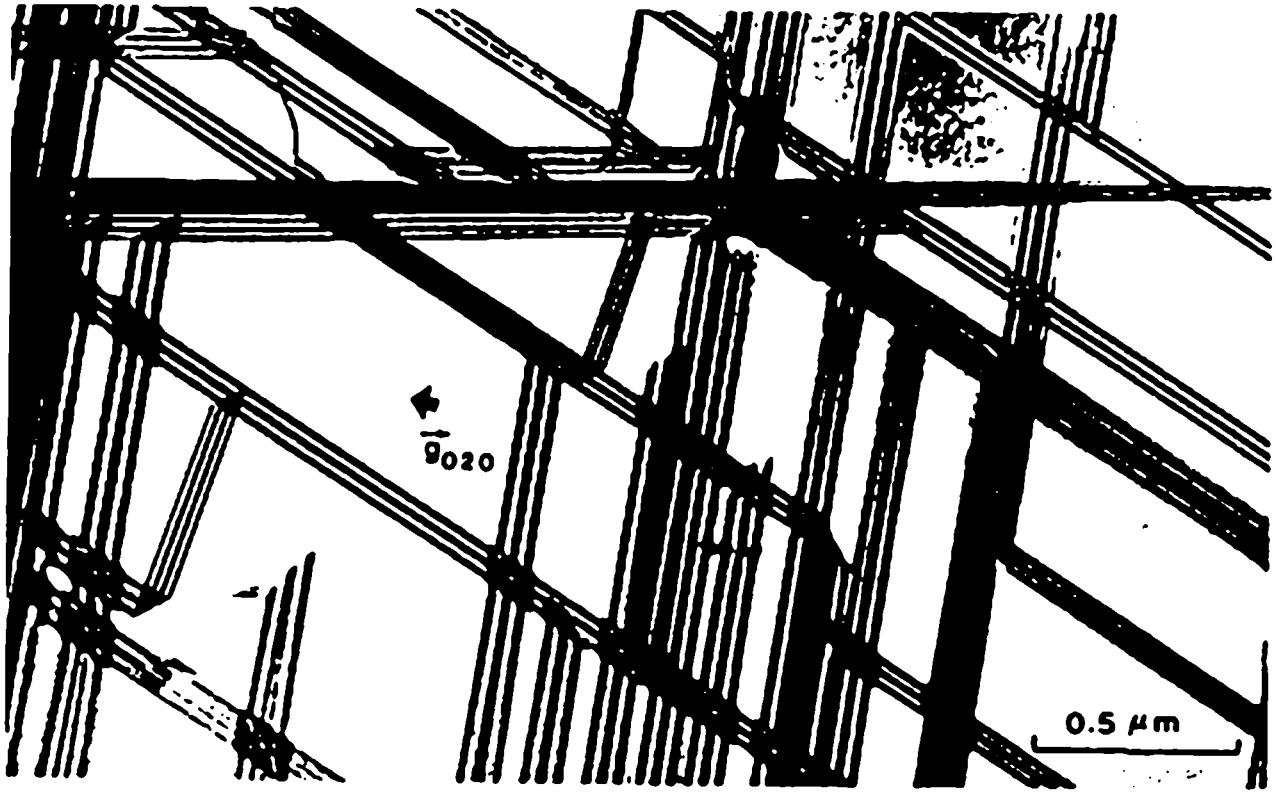

Fig. 8 TEM micrograph showing dense fcc stacking faults and the intersections of stacking faults in the alloy 5 with 4.5%wt nickel after fatigue testing. Beam direction along $[100]_{fcc}$.

two lattices thus have a simple and reproducible orientation relationship which is always observed by appropriate diffraction operation:

$$(111)_{fcc} \| (0001)_{hcp},\ \langle 1\bar{1}0\rangle_{fcc} \| \langle 11\bar{2}0\rangle_{hcp}.$$

The morphology of the interphase boundaries of the fcc to hcp transformation nucleated at the stacking fault intersection sites is different from that of the long straight plate-like structure. It may be concluded that the fcc/hcp boundaries at the intersection nodes are semi-coherent or incoherent considering the existence of a large accommodation strain, as seen in Fig. 3 and 4.

As mentioned above, from the crystallographic point of view, fcc to hcp transformation occurs when the overlapping of stacking faults are formed on the $(111)_{fcc}$ slip planes and two processes are expected for the overlapping of stacking faults: a) regular, and b) irregular overlapping process.

If the hcp crystals are formed by the regular overlapping process, it is expected that they will have the characteristics as following: The hcp plates seldom include stacking faults. Because of the constraint caused by the surrounding matrix, stacking faults in this case are rarely induced in hcp crystals. Moreover, even at the early stage of formation, diffraction spots of hcp crystal appear at the expected sites. However, if the hcp crystals are formed by the irregular overlapping process, they will have the following characteristics: The plates contain a large number of stacking faults in general. In addition, diffraction spots from the fcc matrix are broadened into streaks at first and then pronounced intensity maxima appear on these streaks. These intensity maxima change gradually to regular diffraction spots of the hcp crystal.

The experimental results of the present study, both the examinations of structural morphology of the transformed ε-phase and the SADP diffraction analysis,

confirm that the hcp phase induced by cyclic strain in the fatigued Co-Cr-Mo alloys show the features of the regular overlapping process. Stacking faults inside the transformed ε-plates are seldom seen in all of these figures. And in all cases, diffraction spots from the transformed hcp martensite can be seen clearly at their expected sites, as shown in Fig. 1 and Fig. 5. Therefore, it is considered that the strain-induced hcp martensite in cast Co-Cr-Mo alloys is formed by the regular overlapping process, namely the stacking faults are regularly formed on every second layer of {111} slip planes in the fcc matrix.

The fcc to hcp martensitic transformation is affected significantly by stacking fault energy. Remy et al (7-8) reported that for stacking fault energy values approximately less than 15 ergs/cm^2 the fcc to hcp martensitic transformation could be induced by plastic deformation at room temperature. A higher stacking fault energy value leads to the formation of twins. The base Co-Cr-Mo alloy has a very low stacking fault energy value (about 2 ergs/cm^2) (19) which facilitates the strain induced fcc to hcp transformation during fatigue.

In Tisone's investigation (35), it is reported that the stacking fault energy of Co-base alloy is strongly dependent on alloy's composition, especially nickel content. For an alloy with about 60%at cobalt, its stacking fault energy can be increased dramatically by nickel additions in a range up to about 25%at. In the present study, it is found that the strain induced fcc to hcp martensitic transformation does not occur in the modified alloys with nickel additions of about 4.5%wt and 9.5%wt respectively. This result is consistent with and mainly caused by the effects of nickel additions on the alloy's stacking fault energy.

The strain-induced fcc to hcp martensitic transformation has a considerable influence on the mechanical behaviour of the cast Co-Cr-Mo alloys. Although the $(111)_{fcc}$ faceted fractures have been found to be the dominant fatigue fracture feature in cast Co-Cr-Mo alloy tested at room temperature (37), localized hcp martensite plane faceted fractures on the $(0001)_{hcp}$ basal planes introduced by the strain-induced martensitic transformation are also observed. An improved fatigue property with lower fatigue crack growth rates combined with much better ductility of a mixed fatigue crack mode is obtained by the study of alloying the base alloy with nickel, partly because of the effects of nickel on the alloy's stacking fault energy and furthermore on the strain-induced fcc to hcp transformation. Additionally, it is also found that the fcc to hcp transformation affects the cyclic strain hardening behaviour of the cast Co-Cr-Mo alloy. The result of microhardness measurements proved the presence of a reversed cyclic plastic zone within the monotonic plastic zone as predicted by Rice (40). The reversed cyclic plastic zone is corresponding to the thin layer close to the crack plane where the strain-induced fcc to hcp transformation takes place. This has been discussed in a separate paper.

Conclusions

By transmission electron microscopy study, it is found that the cyclic strain during fatigue at room temperature causes an initial martensitic transformation from fcc phase to a heavily faulted hcp structure in the base cast Co-Cr-Mo alloy and its modified version with no nickel addition. No such transformation has been observed in the modified alloys with nickel additions about 4.5%wt and 9.5%wt respectively.

According to the results of the present study, the strain-induced ε-crystals in the cast Co-Cr-Mo alloy are considered to be formed by the regular overlapping process of stacking faults on every second layer of {111} slip planes in

the fcc matrix. A characteristic fcc/hcp orientation relationship involving a parallelism between close-packed planes and directions is observed as: $\{111\}_{fcc} \| \{0001\}_{hcp}$ and $\langle 1\bar{1}0\rangle_{fcc} \| \langle 11\bar{2}0\rangle_{hcp}$.

A low stacking fault energy facilitates the strain-induced fcc to hcp martensitic transformation in the cast Co-Cr-Mo alloy. Effects of nickel additions on the martensitic transformation are mainly caused by the fact that the stacking fault energy of this Co-base alloy is strongly dependent upon nickel content.

The strain induced fcc to hcp martensitic transformation in the cast Co-Cr-Mo alloy affects the fatigue behaviour, especially the fatigue fracture feature. It helps to strengthen the alloy but also lowers its ductility.

Acknowledgements

The authors would like to express their gratitude to Dr. P. Brøndsted, Metallurgy Department of Risø National Laboratory, who helped them to perform the fatigue testing. They are also grateful to Mrs. A. Steffensen who printed the photographs.

References

1. S. Mahajan, M. L. Green and D. Brasen, Metall. Trans. A, 1977, Vol. 8A, pp.283.
2. G. B. Olson and Morris Cohen, Metall. Trans. A, 1976, Vol. 7A, pp. 1897.
3. E. Votava, Acta Metall. 1960, Vol. 8, pp. 901.
4. W. Bollmann, Acta Metall. 1961, Vol. 9, pp. 972.
5. H. Fujita and S. Ueda, Acta Metall. 1972, Vol. 20, pp. 759.
6. F. Lecroisey and A. Pineau, Metall. Trans. 1972, Vol. 3, pp. 387.
7. L. Remy and A. Pineau, Mater. Sci. Engr. 1976, 26, pp. 123.
8. L. Remy and A. Pineau, Mater. Sci. Engr. 1977, 28, pp. 99.
9. S. Mahajan, D. Brasen and T. Wakiyama, Metallography, 1977, 10, pp. 179.
10. H. J. Kestenbach, Metallography, 1977, 10, pp. 189.
11. P. A. Beaven, P. R. Swann and D. R. F. West, J. Mater. Sci. 1979, 14, pp. 354.
12. Y. Tomota, M. Strum and J. W. Morris, Jr., Metall. Trans. A, 1986, Vol. 17A, pp. 537.
13. R. L. Klueh, P. J. Maziasz and E. H. Lee, Mater. Sci. Engr. A, 1988, 102, pp. 115.
14. S. C. Tjong and N. J. Ho, Mater. Sci. Engr. A, 1988, 102, pp. 125.
15. A. M. Tonejc and V. Krasevec, Metallography, 1988, 21, pp. 41.
16. J. B. Vander Sande, J. R. Coke and J. Wulff, Metall. Trans. A, 1976, Vol. 7A, pp. 389.
17. K. Rajan, Metall. Trans. A, 1982, Vol. 13A, pp. 1161.
18. K. Rajan and J. B. Vander Sande, J. Mater. Sci. 1982, 17, pp. 769.
19. K. Rajan, Metall. Trans. A, 1984, Vol. 15A, pp. 1335.
20. N. C. Dahn, D. Morphy and K. Rajan, Acta Metall. 1984, Vol. 32, pp. 1317.
21. J. W. Christian, Proc. Roy. Soc. 1951, Vol. A206, pp. 51.
22. Z. S. Basinski and J. W. Christain, Phil. Mag. 1953, Vol. 44, pp. 791.
23. B. A. Bilby, Phil. Mag. 1953, Vol. 44, pp. 782.
24. A. Seeger, Z. Metallkde. 1953, 44, pp. 247.
25. A. Seeger, Z. Metallkde. 1956, 47, pp. 653.
26. E. DeLamotte and C. Altstetter, Trans. TMS-AIME, 1969, 245, pp. 651.
27. J. P. Hirth, Fundamental Aspects of Dislocation Theory, J. A. Simmoms, R. DeWit and R. Bullough, Eds. National Bureau of Standards, Washington, D. C. 1970, pp. 547.
28. P. M. Kelly, Acta Metall. 1965, Vol. 13, pp. 635.

29. S. Jana and C. M. Wayman, Metall. Trans. 1970, Vol. 1, pp. 2825.
30. G. B. Olson and M. Cohen, Metall. Trans. A, 1975, Vol. 6A, pp. 791.
31. T. Suzuki, H. Kozima, K. Suzuki, T. Hashimoto and I. Ichihara, Acta Metall. 1977, Vol. 25, pp. 1151.
32. J. W. Brooks, M. H. Loretto and R. E. Smallman, Acta Metall. 1979, Vol. 27, pp. 1829.
33. L. E. Murr, K. P. Staudhammer and S. S. Hecker, Metall. Trans. A, 1982, Vol. 13A, pp. 627.
34. D. C. Cook, Metall. Trans. A, 1987, Vol. 18A, pp. 201.
35. T. C. Tisone, Acta Metall. 1973, Vol. 21, pp. 229.
36. E. K. Koster, A. R. Thölén and A. Howie, Phil. Mag. 1964, 10, pp. 1093.
37. L. Z. Zhuang and E. W. Langer, Metall. Trans. A, 1988, in press.
38. Annual Book of ASTM Standards, Sec. 3, Vol. 03.01, E647-83, 1983, pp. 710.
39. Annual Book of ASTM Standards, Sec. 3, Vol. 03.01, E399-83, 1983, pp. 518.
40. J. R. Rice, ASTM STP 415, 1967, pp. 247.